BBA - Molecular and Cell Biology of Lipids 1864 (2019) 158516

Contents lists available at ScienceDirect

BBA - Molecular and Cell Biology of Lipids

journal homepage: www.elsevier.com/locate/bbalip

Metabolic labelling of choline phospholipids probes ABCA3 transport in lamellar bodies

Yang Li[a], Susanna Kinting[a], Stefanie Höppner[a], Maria Elisabeth Forstner[a], Olaf Uhl[b], Berthold Koletzko[b], Matthias Griese[a,*]

[a] Department of Pediatric Pneumology, Dr. von Hauner Children's Hospital, Ludwig-Maximilians University, German Centre for Lung Research (DZL), 80337 Munich, Germany

[b] Division of Metabolic and Nutritional Medicine, Dr. von Hauner Children's Hospital, Ludwig-Maximilians-Universität München, 80337 Munich, Germany

ARTICLE INFO

Keywords:
ABCA3
Lamellar body
Phospholipids
Metabolic labeling
Transport function

ABSTRACT

In the metabolism of pulmonary surfactant, the ATP-binding cassette sub-family A member 3 (ABCA3) is a crucial protein in the formation of the storage compartment for surfactant, the lamellar body (LB), and the transport of phospholipids in it. Mutations in ABCA3 not only disturb surfactant metabolism but also cause chronic interstitial lung diseases. Assays for ABCA3 transport function are needed to investigate pathophysiology of the mutations and treatment options for the patients.

We metabolically labeled choline (Cho) head phospholipids with the Cho analogue, propargyl-Cho. The universal incorporation of propargyl-Cho was confirmed by mass spectrometry and labeled lipids were visualized in confocal microscopy by click reaction with an azide fluorophore. After pulse-labeling propargyl-Cho labeled lipids accumulated in ABCA3+ vesicles in a time and concentration dependent manner. When treated with the choline kinase inhibitor MN58b during the first 12 h, the lipids intensity inside ABCA3+ vesicles decreased, whereas intensity was unchanged when treated after 12 h. Miltefosine, a substrate of ABCA3, decreased the incorporation of labeled lipids in ABCA3+ vesicles at all time points. The lipids intensity inside the mutated (p.N568D or p.L1580P) ABCA3+ vesicles was decreased compared to wild type, while the intensity outside of vesicles showed no difference.

Propargyl-Cho can metabolically pulse-label Cho phospholipids. Visualization and quantification of fluorescence intensity of the labeled lipids inside ABCA3+ vesicles at equilibrium can specifically assess the transport function of ABCA3.

1. Introduction

Pulmonary surfactant is a critical component at the air liquid interface of the alveoli enabling normal gas-exchange. About 80–90% of surfactant is composed of lipids, including phosphatidylcholine (PC, 70–85%), cholesterol (10–20%), phosphatidylglycerol (10%), a small amount of sphingomyelin (2.3%) and other lipids [1–3]. In alveolar type II (ATII) cells, surfactant lipids are synthesized in the endoplasmic reticulum (ER), then transferred through the Golgi system to the organelles responsible for storage and secretion of surfactant, the so called lamellar bodies (LBs) [1,4]. After secretion of LB content into the alveolar space, surfactant can be recycled by ATII cells or degraded by alveolar macrophages [5].

ATP binding cassette subfamily A member 3 (ABCA3) is responsible for lipid translocation from the cytoplasm into LBs. ABCA3 is localized in the outer membrane of the LBs and also plays a role in the biogenesis of LBs [6–9]. A knock out of ABCA3 in rats caused abnormal genesis or disappearance of LBs in ATII cells [10], whereas its cellular expression induces their formation [9,11–13]. Mutations in ABCA3 may lead to misfolding of the protein which may be retained in the ER, or cause

Abbreviations: ABCA3, ATP-binding cassette sub-family A member 3; LB, lamellar body; Cho, choline; Propargyl-Cho, Propargyl-choline; PC, phosphatidylcholine; lyso-PC, lysophosphatidylcholine; ATII, alveolar type II; CK, choline kinase; chILD, interstitial lung diseases in children; TopF-PC, TopFluor phosphatidylcholine; MLF, miltefosine

* Corresponding author at: Dr. von Hauner Children's Hospital, Division of Pediatric Pneumology, University Hospital Munich, Lindwurmstr. 4, 80337 München, Germany.

E-mail addresses: Yang.Li@med.uni-muenchen.de (Y. Li), Susanna.Kinting@med.uni-muenchen.de (S. Kinting), Stefanie.Hoeppner@med.uni-muenchen.de (S. Höppner), Maria_Elisabeth.Forstner@med.uni-muenchen.de (M.E. Forstner), Olaf.Uhl@med.uni-muenchen.de (O. Uhl), Berthold.Koletzko@med.uni-muenchen.de (B. Koletzko), Matthias.Griese@med.uni-muenchen.de (M. Griese).

https://doi.org/10.1016/j.bbalip.2019.158516
Received 20 June 2019; Received in revised form 21 August 2019; Accepted 26 August 2019
Available online 29 August 2019

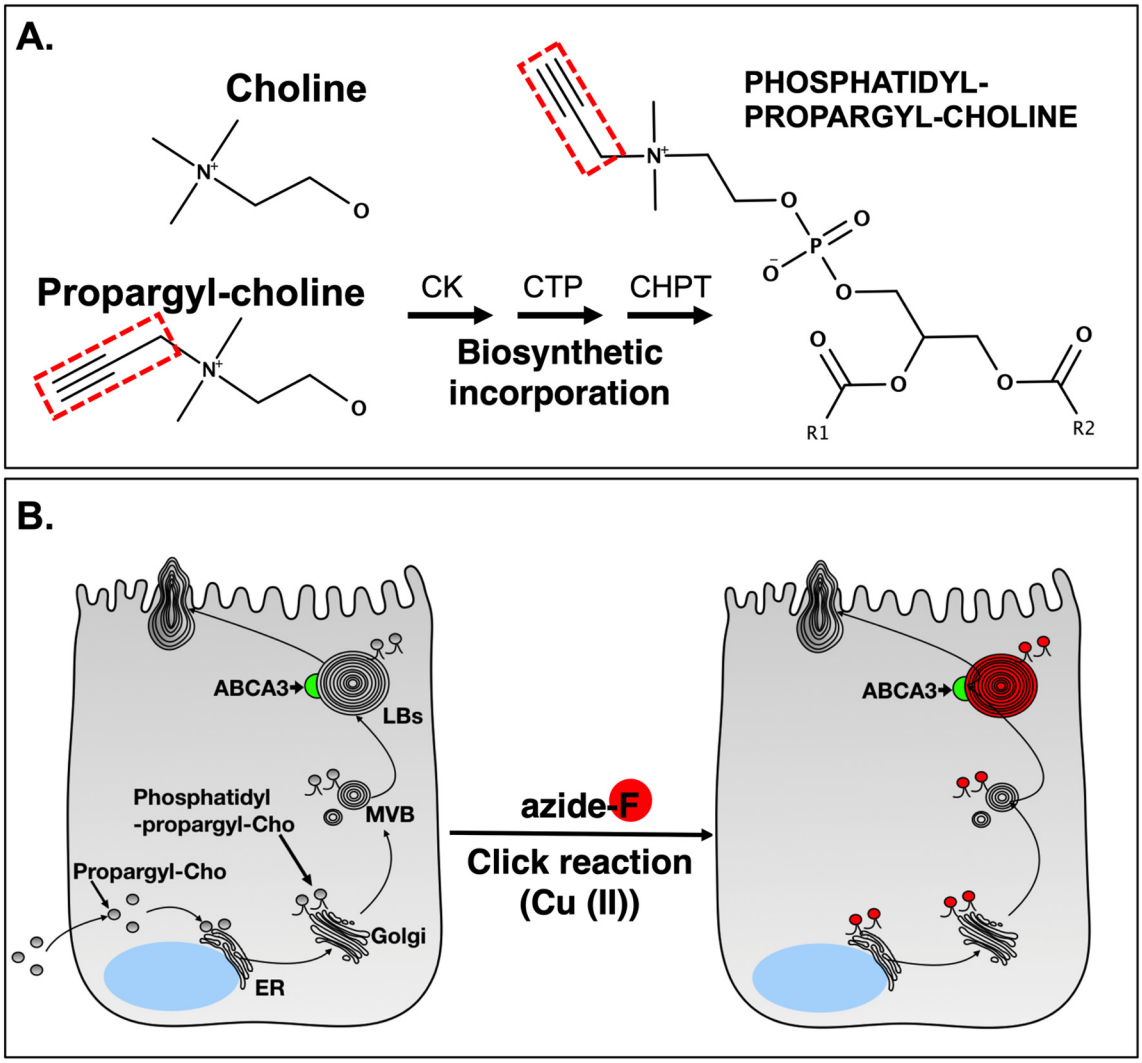

Fig. 1. Propargyl-choline (propargyl-Cho) and click reaction. (A) De novo synthesis of phosphatidyl-propargyl-choline. Replacing one methyl of choline (Cho) by a three-carbon propargyl group (red dot box) forms propargyl-Cho. After its uptake into the cell, propargyl-Cho is incorporated into phosphatidyl-propargyl-Cho by the sequential activity of choline kinase (CK), phosphocholine cytidylyltransferase (CTP) and choline phosphotransferase (CHPT). (**B**) Click reaction to label phosphatidyl-propargyl-Cho. At the end of experiments, propargyl-Cho treated cells were fixed and labeled lipids could react with an azide fluorophore (F) (TAMRA-PEG3-Azide) on the condition of Cu^{2+}. Visualization is then possible by confocal microscopy. ER: Endoplasmic reticulum, MVB: Multi-vesicular body, LB: Lamellar body.

dysfunction of the transporter [7,13,14]. Up to now, > 200 mutations of ABCA3 have been discovered. ABCA3 mutations can cause acute respiratory failure in neonates, as well as interstitial lung diseases in children (chILD) and adults [15–17].

To help patients suffering from diseases caused by ABCA3 mutations, it is urgent to find an effective treatment for restoring ABCA3 function. Recently, we reported that correctors and potentiators originally used for the correction of ABCC7 (CFTR) could rescue the function of certain ABCA3 mutations as well [18,19]. In those experiments TopFluor phosphatidylcholine (TopF-PC) was exposed to the cells in liposomes [20]. Disadvantage of this method is the use of a bulk fluorophore introduced in PC at the expense of one fatty acid, potentially leading to unclear intracellular handling of TopF-PC compared to natural PC.

During normal metabolism and de novo synthesis of PC, extracellular choline (Cho) is taken up by the choline kinase (CK) in the cytosol of ATII cells and transformed to PC by sequential action of choline-phosphate cytidylyltransferase and cholinephospho-transferase (Fig. 1A). Other Cho containing phospholipids like lyso-PC and sphingomyelin are formed by remodeling of PC [1,21].

Propargyl-choline (propargyl-Cho) is a small choline analogue utilized to metabolically label Cho-phospholipids via their cellular synthetic pathway (Fig. 1A). One methyl of choline is replaced by a three-carbon propargyl group to form propargyl-Cho. Previously metabolic handling of propargyl-Cho corresponding to that of Cho was shown in mammalian and plant cells [22,23]. In this study we metabolically labeled Cho containing lipids with propargyl-Cho and established a new assay to quantify the Cho containing phospholipids transport function of ABCA3.

2. Methods

2.1. Site directed mutagenesis and generation of stable cells

A549 cells stably expressing HA-tagged ABCA3 protein (ABCA3-HA) were established as previously described [12]. Briefly, ABCA3-N568D (c. 2886A > G; CAA/CGA) or ABCA3-L1580P point mutations (c.5923 T > C; CTG/CCG) were introduced into the pT2/HB-CMV-hABCA3-HA-PGK-Puromycin vector with Q5® Site-Directed Mutagenesis Kit (New England Biolabs, Ipswich, MA). Using the Sleeping Beauty

transposon system, vectors were stably transfected into A549 cells. Single cells were seeded in 96-well plates and selected with puromycin containing medium. The mRNA expression of ABCA3 was examined by qPCR. Rat anti HA (Roche, Germany) was used as first antibody in immunoblot and confocal microscopy for analyzing the ABCA3 protein expression.

2.2. Addition of propargyl-choline to the medium and click reaction

Bromo salt of propargyl-Cho (N-(2-Hydroxyethyl)-*N*,*N*-dimethyl-2-propyn-1-aminium bromide) was purchased from Jena Bioscience (Cat. No. CLK-066) and a stock solution was prepared by adding 156.7 µl of PBS to the solid. The final propargyl-Cho concentration was 50 mM. In each experiment, the cells were seeded in µ-slides (IBIDI, Martinsried, Germany) with a concentration of 200,000 cells/ml and incubated at 37 °C for 24 h. Afterwards the cells were cooled down to 4 °C for 15 min and propargyl-Cho solved in OptiMEM (ThermoFisher, Waltham, USA) was added for 30 min. First, in concentration-dependent experiments, a different range of propargyl-Cho was used to optimize the working concentration for confocal microscopy. A concentration of 125 µM was chosen for all other experiments. In the ATPase inhibition experiment, cells were treated with 12.5 mM orthovanadate (Sigma, Taufkirchen, Germany) for 2 h after labeling and then incubated for 22 h.

To further explore the synthesis and transportation of labeled lipids, 10 µM of miltefosine (Cayman chemical, Michigan, USA) or 10 µM of MN58b (AOBIOUS, Massachusetts, USA) dissolved in dimethyl sulfoxide (DMSO, Sigma) was added after propargyl-Cho incubation at 0 h or 12 h. In the washout experiments, chemicals were washed off with 37 °C PBS (Sigma) after 12 h and incubated with OptiMEM for another 12 h. The fixation of the cells and the immunofluorescence staining of ABCA3-HA protein was done as previously described [20].

Prior to performing click chemistry reaction (Fig. 1B), the fixed samples were treated with 1% saponin (Roth, Mannheim, Germany) to permeabilize cell membranes. After washing with a buffer containing 3% bovine serum albumin (BSA, Sigma) and 0.1% saponin in PBS, the cells were treated with 20 µM of 5-carboxytetramethylrhodamine (TAMRA)-PEG3-Azide (Baseclick GmbH, Neuried, Germany) in DMSO, 128 µM Tris((1-hydroxy-propyl-1H-1,2,3-triazol-4-yl) methyl) amine (THPTA, Baseclick GmbH), 1 mM CuSO4 and 1.2 mM sodium ascorbate (Sigma) were mixed up in PBS with 0.01% BSA and 0.1% saponin. The azide-mixture was added to cells with phosphatidyl-propargyl-Cho, incubated for 30 min and washed nine times to remove excess or water soluble propargyl metabolic intermediates with PBS containing 3% BSA and. 0.1% saponin [22].

2.3. Cytotoxicity assay

Wild type (WT) A549 ABCA3-HA cells were seeded in 96-well plates at 50,000 cells per well. After 24 h, 125 µM propargyl-Cho in phenol red free Roswell Park Memorial Institute (RPMI, Gibco, Darmstadt, Germany) medium was added and washed out after 30 min at 4 °C. Hereby WT cells without propargyl-Cho were taken as control. Cell viability was tested by 2,3-Bis-(2-Methoxy-4-Nitro-5-Sulfophenyl)-2H-Tetrazolium-5-Carboxanilide (XTT, Sigma) in the presence of phenazine methosulphate (PMS, Sigma).

2.4. Immunostaining and confocal microscopy

ABCA3-HA was labeled with anti-HA antibody (Sigma, 1:200), washed with 3 times of PBS, then stained with AlexaFluor-488 conjugated second antibody (ThermoFisher, 1:200). Calnexin - (Santa Cruz Biotechnology, Texas, USA, 1:200), GM130 - (Santa Cruz Biotechnology, 1:200) and EEA1 - (BD Biosciences, New Jersey, USA, 1:200) specific antibodies in combination with according AlexaFluor conjugated second antibodies were used for endoplasmic reticulum and Golgi apparatus staining. Fixed and stained cells were mounted prior to microscopy with a Carl Zeiss LSM800 system. Propargyl-Cho with TAMRA fluorescein was visualized by excitation filter setting at 561 nm. ABCA3-HA protein stained with Alexa Fluorophore 488 was excited at 488 nm. Laser power, pinhole, digital gains and offsets remained the same for TAMRA in all confocal images. For fluorescence intensity calculation, z-stacks with 5 pictures in 0.4 µm intervals were obtained for each chamber. Experiments were performed in duplicates, obtaining three z-stacks per well.

2.5. Quantification of fluorescence intensity

The quantification of fluorescence intensity inside the vesicles was done as previously described [20]. The Fiji-Plugin "Particle_in_Cell-3D" [24] was used for fluorescence measuring. Fluorescence intensity in twenty randomly chosen vesicles was analyzed with the plugin. Four parameters were analyzed: fluorescence intensity in all selected vesicles, fluorescence intensity in filled vesicles, percentage of filled vesicles and vesicle volume. For analyzing the fluorescence intensity in the cytosol outside of vesicles, twenty regions of interest with the same size (1 μM^2) were randomly selected without overlay with any ABCA3 + vesicles (Fig. S1).

2.6. Phosphatidylcholine mass spectrometry

The phospholipids were extracted by adding methanol to the cells. After extraction and centrifugation an aliquot of the supernatant was injected into a triple quadrupole mass spectrometer (4000QTRAP, AB Sciex Germany GmbH, Darmstadt, Germany) by continuous direct injection at a low rate of 10 µl/min. The mass spectrometer was operated in precursor-ion-scan, selecting for a target fragment of m/z = 184 Da for phosphatidylcholines or m/z = 208 Da for propargyl-Cho in the mass range from 400 to 1000 Da as described [22].

2.7. Statistics

Means and standard deviations of lipids intensities, percentage of filled vesicles and volume of vesicles were calculated with Excel. Significance of differences between two groups were calculated with student *t*-test. One-way or two-way ANOVA with Tukey, Dunnett or Sidak correction of multiple comparisons test were conducted among more than two groups with GraphPad Prism.

3. Results

3.1. Propargyl-Cho incorporated into choline phospholipids in A549 cells

First, we determined whether propargyl-Cho was incorporated into Cho phospholipids within our A549 ATII cell model stably transfected with ABCA3-HA. Mass spectrometry of propargyl-Cho head phospholipids detected at m/z 208 in labeled cells showed similar chromatography pattern with Cho head phospholipids at m/z 184 in untreated cells (Fig. 2A). Incorporation of propargyl-Cho into sphingomyelins was also identified (data not show). Afterwards, labeled cells were processed with click chemistry reaction to attach fluorescent azide and were visualized by confocal microscopy. Lipids signal was apparent inside ABCA3 + vesicles and cell plasma, without association to the nuclei (Fig. 2B). Labeled lipids could also be observed outside of vesicles in the cytosol. Co-localization of lipids and the markers of ER, Golgi and early endosomes were found (Fig. S3). Propargyl-Cho labeling was not cytotoxic to cells (Fig. S2A).

3.2. Concentration dependent incorporation of propargyl-Cho in WT ABCA3-HA cells

The average fluorescence intensities in the analyzed vesicles increased accordingly to the concentrations of propargyl-Cho (Fig. 3A).

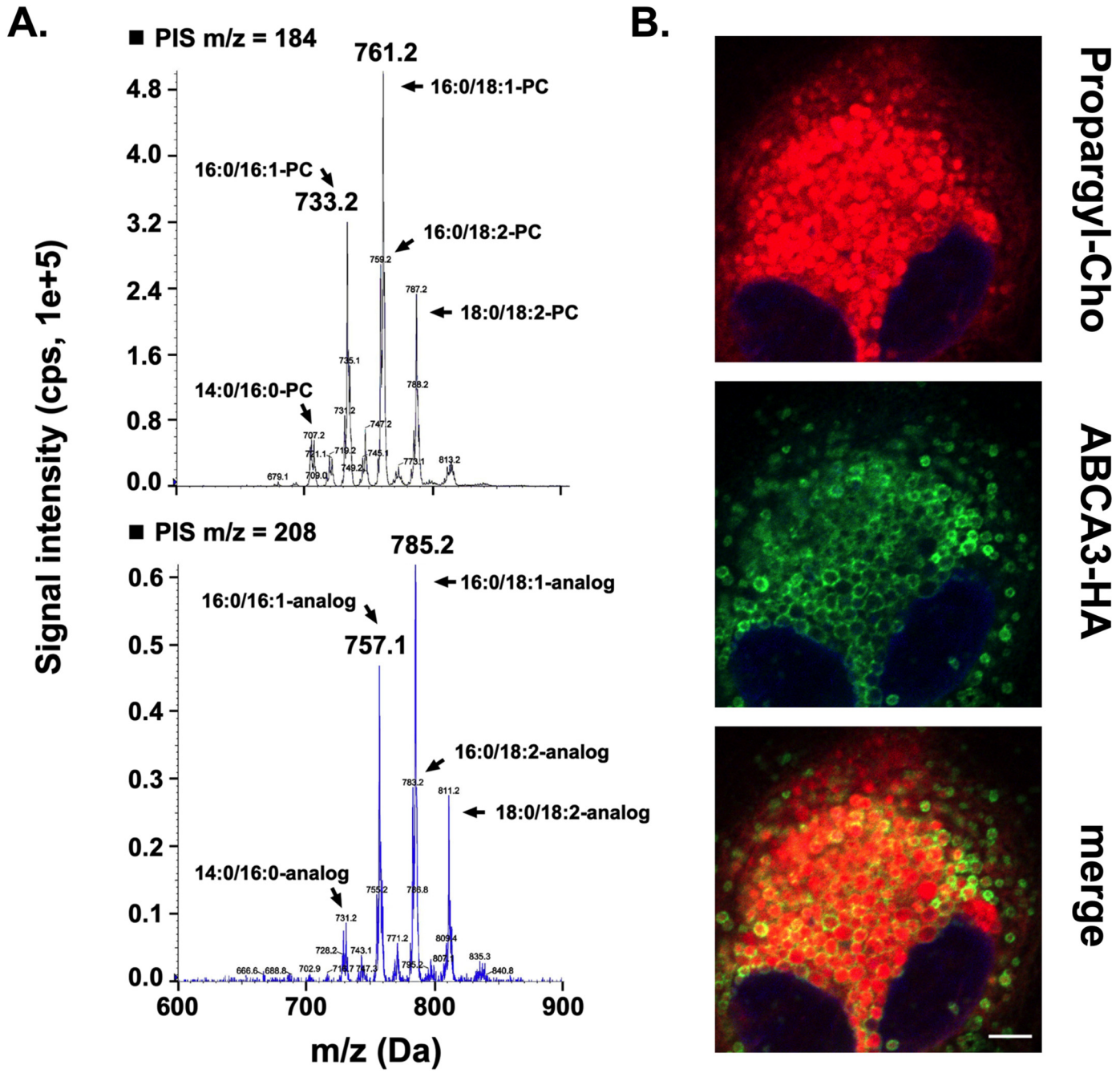

Fig. 2. Incorporation of propargyl-Cho into Cho phospholipids in A549 WT ABCA3-HA cells. (A) Lipid spectrum of cells treated with propargyl-Cho. Upper panel: molecular species of phosphatidylcholine. Lower panel: phosphatidyl-propargyl-Cho. Specific mass peaks of lipid species as examples of successful incorporation were marked by arrows. PIS: precursor-ion-scan. Cps: counts-per-second. (B) Confocal microscopy images of propargyl-Cho treated cells after click reaction. ABCA3-HA protein was stained with anti-HA antibody and according Alexa Fluor 488 secondary antibody. The fluorescence intensity of propargyl-Cho inside ABCA3+ vesicles was uniform and strong, while lipids signal outside of vesicles in the cytoplasm was weak but non-negligible. Scale bar: 5 μm.

Average intensity in filled vesicles treated with 50 μM propargyl-Cho was 34.1% of that with 250 μM propargyl-Cho (Fig. 3B). At lower concentration of propargyl-Cho, fluorescence intensity outside of ABCA3+ vesicles appeared to be lower than inside, however not at high concentration (Fig. 3C). 99.8% of chosen vesicles were filled with labeled lipids when treated with 250 μM propargyl-Cho for 24 h, but only 63.9% for 50 μM propargyl-Cho (Fig. 3D). Increasing concentration of propargyl-Cho did not influence the volume of ABCA3+ vesicles in the cells (Fig. 3E).

3.3. Time dependent incorporation of propargyl-Cho in WT ABCA3-HA cells

When treated with 125 μM propargyl-Cho, the lipid fluorescence intensity in ABCA3+ vesicles increased gradually within 24 h and remained stable over 48 h (Fig. 4A, B). At this concentration of propargyl-Cho the accumulation of fluorescence intensity was higher inside than outside the ABCA3+ vesicles for up to 48 h (Fig. 4C). After 24 h, lipids could be easily observed within the ABCA3+ vesicles (white arrow, Fig. 4A). The percentage of filled vesicles similarly increased over time reaching a plateau after 24 h, when all chosen vesicles were filled with

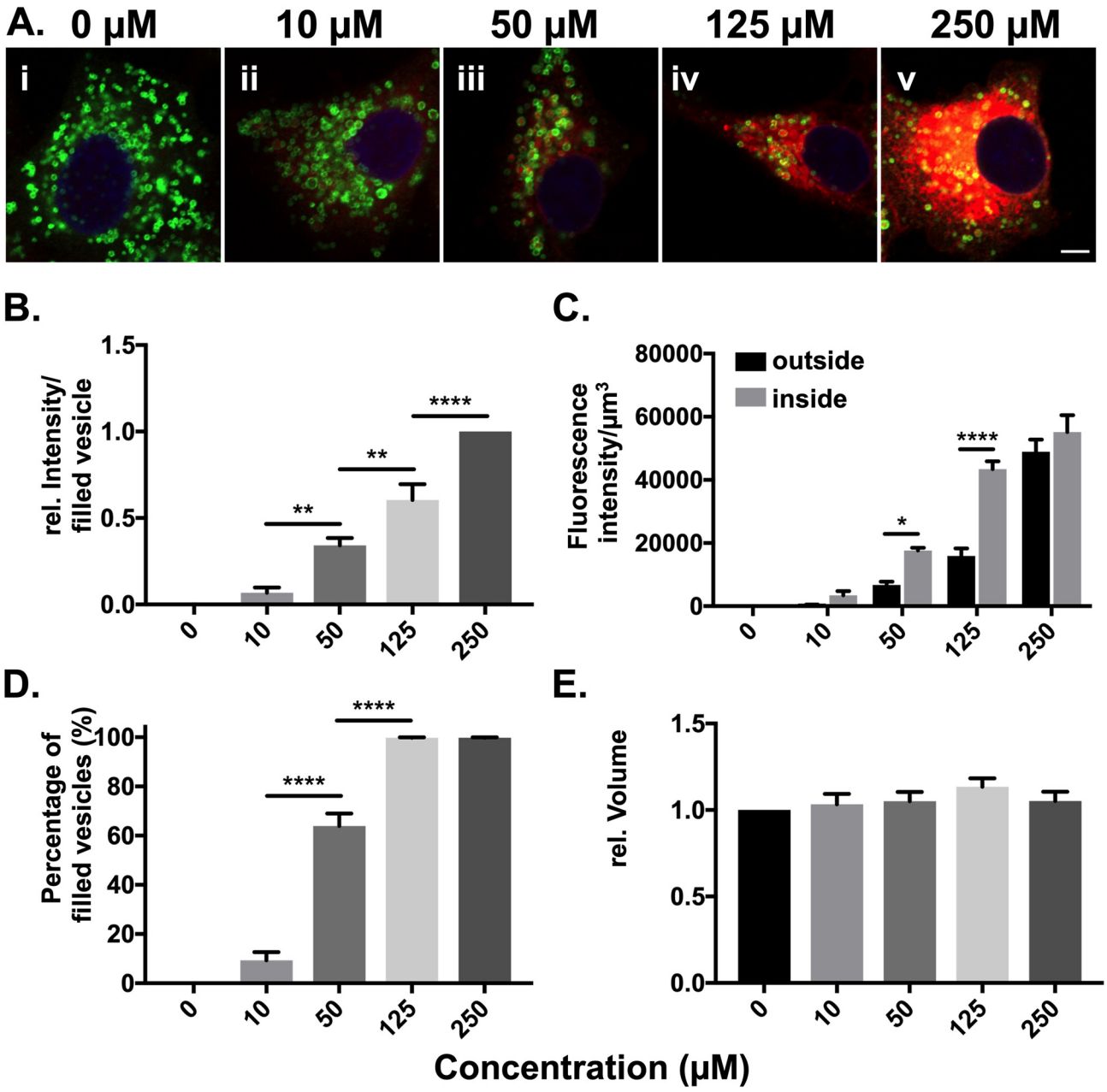

Fig. 3. Concentration dependent incorporation of propargyl-Cho. (A) A549 cells were pulse-labeled with varying concentration of propargyl-Cho. The lipids intensity in cells (both inside and outside of ABCA3+ vesicles) increased with increasing propargyl-Cho concentration. Scale bar: 5 μM. (B) Relative fluorescence intensity in filled vesicles. The fluorescence intensities at 10 μM and 50 μM propargyl-Cho were 6.8% and 34.1% of the intensity at 250 μM respectively. (C) Fluorescence intensity inside and outside of vesicles. Difference between intensities inside and outside of the vesicles only existed when cells were treated with 50 μM propargyl-Cho. (D) The percentage of filled vesicles increased with higher concentration of propargyl-Cho. (E) The ratio of volume was compared to the mean volume of untreated cells. $^{*}P < 0.0332$, $^{**}P < 0.0021$, $^{***}P < 0.0002$, $^{****}P < 0.0001$.

detectable labeled choline phospholipids. Vesicle volume did not change with time (Fig. 4D, E).

3.4. Cho phospholipids in the cells decrease when treated with ATPase inhibitor

We examined if the transport of phosphatidyl-propargyl-Cho into LBs was ATP dependent. After treatment with the ATPase inhibitor orthovanadate, the fluorescence intensity in filled vesicles was decreased compared to non-treated cells while the volume of the organelles stayed the same (Fig. 5). The lipids intensity outside of vesicles decreased also. (Fig. 5B).

3.5. Fluorescence intensity inside vesicles indicates the transport function of ABCA3

The time curve of propargyl-Cho accumulation in ABCA3+ vesicles must reflect both the synthesis and transport process of labeled lipids. To assess the contribution of these two processes over time, we used a choline kinase inhibitor MN58b [25], or miltefosine (MLF), which was determined to be a substrate of ABCA3 in human macrophages [26] (Fig. 6A). Both the presence of MLF or MN58b for 24 h reduced by 68% phosphatidyl-propargyl-Cho in ABCA3+ vesicles compared to control. Lipid intensity and the percentage of filled vesicles were irreversibly decreased after washing out of MN58b at 12 h. While in the case of MLF, washing out restored vesicles filling with fluorescent lipids

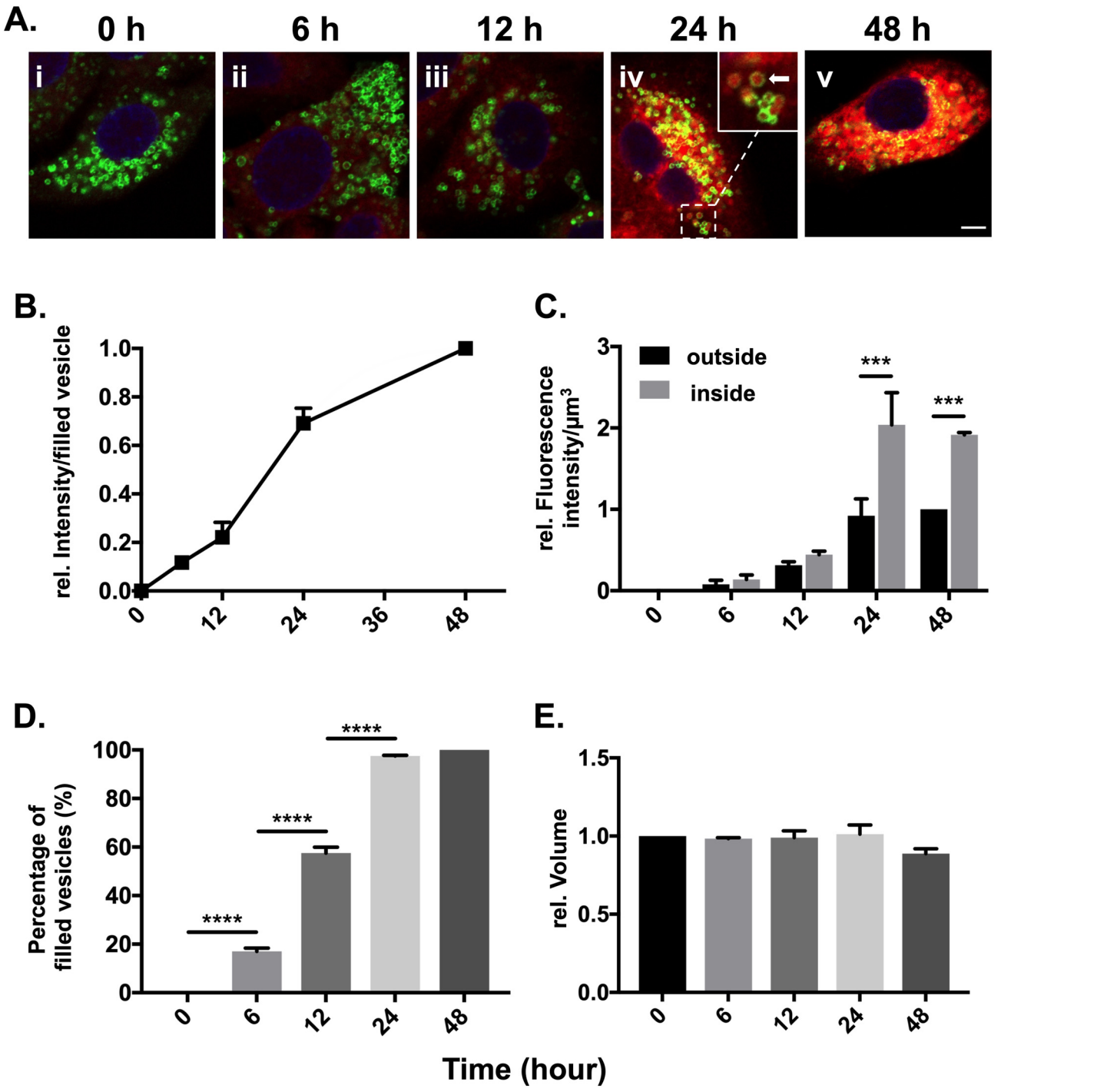

Fig. 4. Time dependent incorporation of propargyl-Cho. (A) A549 cells were treated with the same concentration of propargyl-Cho (125 µM) but incubated for different time courses. At 24 h, lipids accumulation in ABCA3 + vesicles could be observed as shown with white arrow (iv). Scale bar: 5 µM. (B) The lipids intensity in the vesicles increased from 12 to 24 h. Measured intensity at 48 h was set to 1. (C) The lipids intensity outside and inside of the vesicles changed over time. Intensity outside of vesicles at 48 h was set as 1. Higher intensities inside ABCA3 + vesicles than outside was observed after 24 h. (D) The percentage of filled vesicles increased over time. All analyzed vesicles were filled with labeled lipids after 24 h. (E) The vesicles volume did not change during the time course.

(0–12 h vs. 0–24 h, Fig. 6). Addition of MN58b after 12 h did not influence fluorescence intensity and portion of filled vesicles anymore (12–24 h MN58b). MLF treatment from 12 to 24 h however reduced fluorescence intensity inside vesicles to 26% of the control. The addition of these two compounds did not influence the vesicle volume. The concentrations of MLF and MN58b used in the experiments were not toxic for the cells (Fig. S2B). These data suggested that inhibition of Cho phospholipids synthesis during the first 12 h after pulse-labeling reduced total amount of labeled PC and does not play a role during the later phase, when primarily lipids uptake in ABCA3 + vesicles occurs.

3.6. Deviation of transport function between N568D, L1580P and WT ABCA3

To further differentiate ABCA3-dependent phospholipid transport function, we introduced site directed mutations into ABCA3. p.N568D is a mutant located in the Walker A motif of the nucleotide binding domain 1 (NBD1), and p.L1580P is located close to NBD2. Both

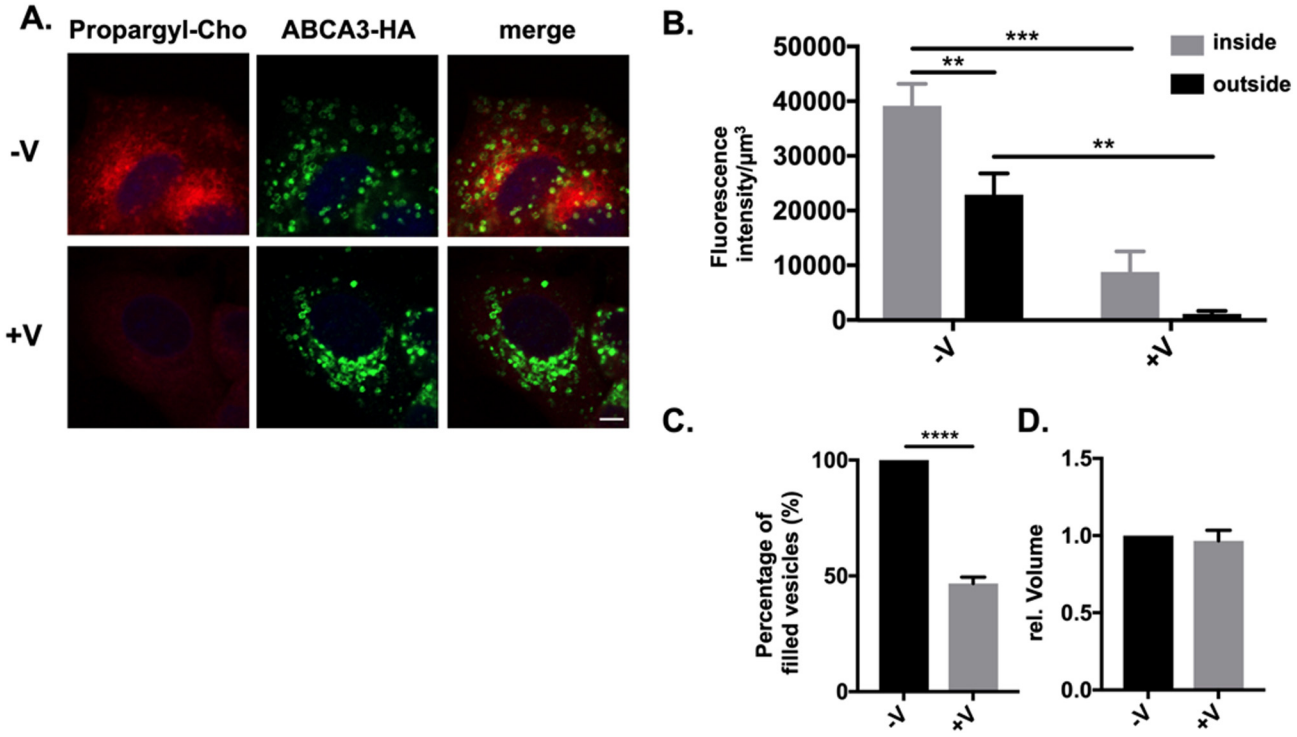

Fig. 5. Phosphatidyl-propargyl-Cho in cells decreased when treated with ATPase inhibitor. (A) 2 h after pulse-labeling with 125 µM propargyl-Cho, cells were incubated with or without 12.5 mM orthovanadate for 22 h. −V, without orthovanadate. +V, with orthovanadate. Scale bar: 5 µM. (B) The fluorescence intensity was decreased inside and outside the vesicles when treated with orthovanadate. (C) The percentage of filled vesicles was reduced by 50% when treated with orthovanadate. (D) Vesicle volume did not differ between orthovanadate-treated or non-treated cells.

mutations were found in patients who suffered from neonatal surfactant deficiency [27] and dependently reported to impair ATPase function of the transporter [9,11]. Both the ABCA3-N568D and ABCA3-L1580P vesicles were smaller than those in WT ABCA3 expressing cells (Fig. 7E). The time curve of incorporation and transportation of propargyl-Cho lipids into ABCA3+ vesicles were similar between WT and mutant ABCA3 up to 12 h. In mutated cells almost no further accumulation of phosphatidyl-propargyl-Cho in ABCA3+ vesicles occurred, whereas in WT intensity increased further (Fig. 7A, B). After 24 h, fluorescence intensities between WT or mutant vesicles did not differ outside of ABCA3 + vesicles, whereas intensity inside was higher in WT than mutants (Fig. 7C).

4. Discussion

Metabolic labeling of the Cho head group phospholipids with propargyl-Cho and its visualization by click chemistry at certain time points (here after 24 h) represents a simple, direct and non-radioactive method to specifically analyze the role of ABCA3 transport function in Cho phospholipid metabolism. We found that fluorescence intensity inside vesicles indicated the transport function of ABCA3 specifically, and helped to define the transport function deviation of two ABCA3 mutants from the WT.

In biochemical studies of lung phosphocholine physiology, various choline analogues have been investigated for metabolic labeling. For example, [^{3}H] choline was utilized as a precursor to label PC for studying the synthesis [28], transport [29], secretion and clearance of surfactant in ATII cells [30,31]. Unlike this Cho analogue, propargyl-Cho is non-radioactive and has been utilized in Cho phospholipids labeling in vitro in cell models, in vivo in mouse models, ex vivo in oral biopsy tissue [22,23,32], and also in plants and *Streptococcus pneumoniae* [33,34]. Propargyl-Cho showed incorporation into phospholipids efficiently in all cases, without interfering normal lipid metabolism or cell physiology. Here we confirmed the integration of propargyl-Cho by lipids mass spectrometry. Similarly, fluorescence intensities in ABCA3+ vesicles in cells treated with 250 µM propargyl-Cho were 2.9-fold higher than in cells treated with 50 µM. This is in accordance with the results from Jao et al., who described an increase of replaced Cho detected by mass spectrometry less than three times with five times the amount of propargyl-Cho.

Since choline phospholipids are important components for all biomembranes in the cell, the background interference from labeling of Cho head phospholipids of other membranes in the cell should not be ignored (Fig. S1). Besides consistent settings for fluorescence acquiring at confocal microscopy, assessment of propargyl-Cho lipids intensity outside of ABCA3+ vesicles while analyzing the intensity changes inside of vesicles helped to minimize the interference of background staining.

During pulse-labeling with propargyl-Cho, the Cho analogue was transported actively and rapidly into the cells and used for newly synthesized lipids. Thus, we hypothesized that the phosphatidyl-propargyl-Cho inside ABCA3+ vesicles at 24 h was synthesized during the previous 12 h. To verify this, we inhibited the phosphorylation of propargyl-Cho with the specific CK inhibitor, MN58b [25,35]. Although in Kennedy pathway of PC synthesis the activation of phosphocholine into cytidine-diphosphocholine by phosphocholine cytidylyltransferase is the rate limiting step, the phosphorylation of Cho by choline kinase could also regulate PC biosynthesis [36,37]. Inhibition of choline kinase 12 h after propargyl-Cho labeling did not influence the final amount of lipids transported into ABCA3+ vesicles (Fig. 6). Thus, intensity changes specifically quantified in ABCA3+ vesicles at 24 h may represent transport function of the transporter alone.

Furthermore, we found that Cho phospholipids inside ABCA3+ vesicles were decreased in ABCA3+ vesicles of p.N568D and p.L1580P mutants, but not in the cell plasma. These results also demonstrate that phosphatidyl-propargyl-Cho is specifically transported into vesicles by ABCA3, since the ATP-dependent transport activity was reduced in mutants of ABCA3. Whereas Matsumura et al. previously assessed and

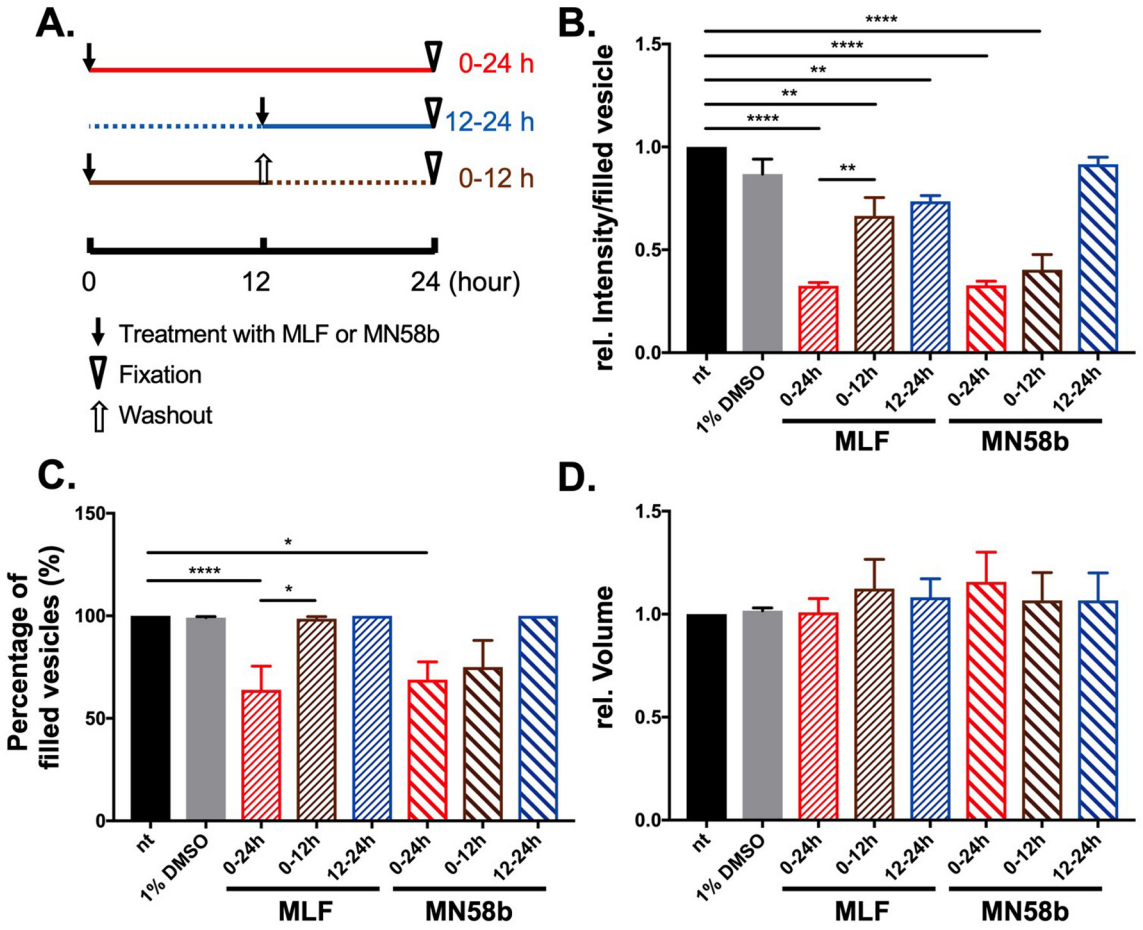

Fig. 6. Fluorescence intensity inside vesicles decreased when treated with ABCA3 substrate miltefosine (MLF) or choline kinase inhibitor MN58b. (A) Workflow. Cells were treated with 10 μM MLF or MN58b at 0 h or 12 h and fixed at 24 h after the addition of propargyl-Cho (0–24 h, 12–24 h). In washout experiments, chemicals were washed out with PBS after 12 h (0 – 12 h). (B, C) In the presence of MLF, the lipids intensity in vesicles decreased to 32.5% (0–24 h) and 73.5% (12–24 h) of non-treated (nt). When MLF was washed off after 12 h, lipids intensity was decreased to 66.5% (0–12 h). Treatment with MN58b decreased the intensity to 32.7% of nt during 0–24 h, while it had no effects during 12–24 h. Neither the lipids intensity nor the percentage of filled vesicles increased after washing out of MN58b (0–12 h). (D) The volume of vesicles was unchanged between treated and control groups.

showed that ATP hydrolysis and binding activity of p.N568D and p.L1580P mutants were decreased [11], we directly demonstrated impaired Cho phospholipids transport function of these two mutants.

Our results are comparable to those studies where TopF-PC labeling was used [20]. Both methods were designed to quantify the PC incorporated by ABCA3 in lamellar bodies and give similar results. The incorporation of propargyl-Cho and TopF-PC into ABCA3+ vesicles were time and concentration dependent with an identical pattern, and the analog phospholipids inside ABCA3+ vesicles decreased when a damaging mutation was introduced. However, some facts of TopF-PC labeling should not be ignored. 1) Unclear metabolic labelling of TopF-PC inside the cells. The molecular weight of TopF-PC is 910 g/mol, while that of normal PC in surfactant is between 700 and 800 g/mol [16]. Whether the larger size and the structure difference from unlabeled PC would influence the PC metabolism remains to be elucidated. 2) Labeled lipids were supplied as part of liposomes to the cells. How these are internalized and routed to their biopath in the cells need to be clarified. 3) Whether the fluorophore labeled lipids transported by ABCA3 are directly coming from the liposomes or from digested and remodified lipids is unknown. Metabolic labeling of Cho phospholipids circumvents some of these problems.

As it is necessary to fix the cells before conducting the azide-fluorophore click reaction, it is not possible to observe the movement of labeled lipids between membranes with live cell imaging. While TopFluor phospholipids were employed to study the movement of phosphatidylserine in the plasma membrane [38], combining that label with the methods used here, could be a complementary option in the future.

Due to the lack of primary human alveolar type II cell cultures and antibodies for untagged ABCA3 protein immunofluorescence staining, we used A549 cells stably over expressing ABCA3-HA. Whereas the genotype background and cellular phenotype of A549 cells are different from ATII cells [39,40], there was no evidences regarding an ABCA3-driven alteration of the biogenesis of the lamellar bodies, and their morphological appearance. Isolated ATII cells or human induced pluripotent stem cells (IPS) likely are better models to investigate the maturation, secretion and recycling of surfactant and lamellar bodies in the future. Further exploring the role of ABCA3 for the transport of cholesterol, phosphoethanolamine and other non-choline phospholipids of interest necessitate the utilization of additional labels.

Apart from interstitial lung diseases, ABCA3 was also found to play a role in drug resistance in leukemia and lymphoma [41–43]. Incubation with different cytostatic drugs led to an up-regulation of ABCA3 expression in human leukemia cells [41]. Our data shows that miltefosine, a previously reported potential substrate of ABCA3 [26], could competitively inhibit the lipid transport function of ABCA3 and as such way might be useful in cancer treatment. As miltefosine is available as oral drug for treatment of cutaneous leishmaniasis, it could be investigated as an adjunct treatment in drug resistant leukemia.

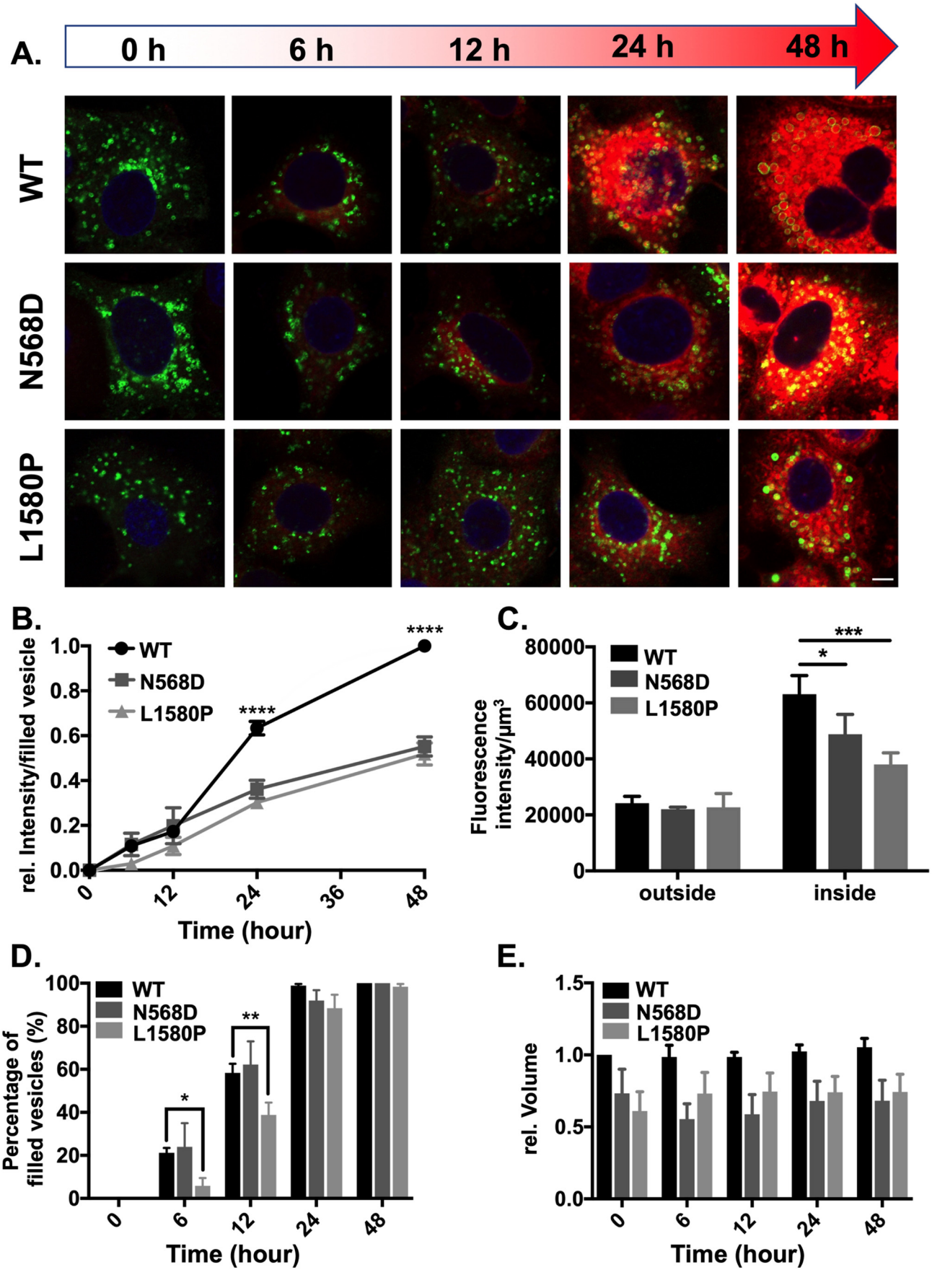

(caption on next page)

Fig. 7. N568D, L1580P ABCA3 showed decreased lipid transport function. (A) p.N568D, p.L1580P and WT ABCA3-HA expressing cells were seeded and treated with 125 μM propargyl-Cho. Scale bar: 5 μM. (B) Time curve of fluorescence intensity in WT and mutant ABCA3+ vesicles. Lipid intensity in WT ABCA3-HA at 48 h was set to 1. In the first 12 h, the fluorescence intensity showed no difference between WT and mutants. After 24 h, intensity in the vesicles of mutant cells was about 50% of that in WT ABCA3 expressing cells. (C) Propargyl-Cho lipids intensities inside and outside of the vesicles in the three cell lines at 24 h. Although the intensity inside the vesicles of mutant cells was lower than in WT ABCA3 cells, the intensity outside of the vesicles showed no difference. (D) After 24 h, almost all vesicles were filled with labeled lipids both in WT and mutants. (E) Vesicles volume of mutants was consistent over time and smaller than WT.

5. Conclusion

Here we provided a novel assay for the quantification of ABCA3 transport function in the Cho phospholipid metabolism of LBs by using the fluorescence intensity of propargyl-Cho labeled lipids inside ABCA3+ vesicles. The method also allows the analysis of spatial distribution of metabolically labeled Cho phospholipids in cellular organelles.

Transparency document

The Transparency document associated with this article can be found, in online version.

Acknowledgement

Supported by the Deutsche Forschungsgemeinschaft (grant number Gr 970/8-1), and Ludwig-Maximilians-Universität München - China Scholarship Council (LMU-CSC) Scholarship Program (grant to YL). Additional financial support for mass spectrometric analyses was provided by the European Research Council Advanced Grant META-GROWTH ERC-2012-AdG-no.322605 and the German Research Council, INST 409/224-1 FUGG.

Appendix A. Supplementary data

Supplementary data to this article can be found online at https://doi.org/10.1016/j.bbalip.2019.158516.

References

[1] J.J. Batenburg, Surfactant phospholipids: synthesis and storage, Am. J. Phys. 262 (4) (1992) L367–L385 Pt 1.
[2] M. Agassandian, R.K. Mallampalli, Surfactant phospholipid metabolism, Biochim. Biophys. Acta 1831 (3) (2013) 612–625.
[3] M. Griese, et al., Quantitative Lipidomics in Pulmonary Alveolar Proteinosis [published online ahead of print April 19, 2019], Am. J. Respir. Crit. Care Med. (2019), https://doi.org/10.1164/rccm.201901-0086OC.
[4] R. Veldhuizen, F. Possmayer, Phospholipid metabolism in lung surfactant, Subcell Biochem 37 (2004) 359–388.
[5] J.R. Wright, Clearance and recycling of pulmonary surfactant, Am. J. Phys. 259 (2 Pt 1) (1990) L1–12.
[6] G. Yamano, et al., ABCA3 is a lamellar body membrane protein in human lung alveolar type II cells, FEBS Lett. 508 (2) (2001) 221–225.
[7] N. Cheong, et al., Functional and trafficking defects in ATP binding cassette A3 mutants associated with respiratory distress syndrome, J. Biol. Chem. 281 (14) (2006) 9791–9800.
[8] N. Ban, et al., ABCA3 as a lipid transporter in pulmonary surfactant biogenesis, J. Biol. Chem. 282 (13) (2007) 9628–9634.
[9] Y. Matsumura, et al., ABCA3-mediated choline-phospholipids uptake into intracellular vesicles in A549 cells, FEBS Lett. 581 (17) (2007) 3139–3144.
[10] N. Cheong, et al., ABCA3 is critical for lamellar body biogenesis in vivo, J. Biol. Chem. 282 (33) (2007) 23811–23817.
[11] Y. Matsumura, et al., Characterization and classification of ATP-binding cassette transporter ABCA3 mutants in fatal surfactant deficiency, J. Biol. Chem. 281 (45) (2006) 34503–34514.
[12] T. Wittmann, et al., Tools to explore ABCA3 mutations causing interstitial lung disease, Pediatr. Pulmonol. 51 (12) (2016) 1284–1294.
[13] U. Schindlbeck, et al., ABCA3 missense mutations causing surfactant dysfunction disorders have distinct cellular phenotypes, Hum. Mutat. 39 (6) (2018) 841–850.
[14] Y. Matsumura, N. Ban, N. Inagaki, Aberrant catalytic cycle and impaired lipid transport into intracellular vesicles in ABCA3 mutants associated with nonfatal pediatric interstitial lung disease, Am J Physiol Lung Cell Mol Physiol 295 (4) (2008) L698–L707.
[15] F. Flamein, et al., Molecular and cellular characteristics of ABCA3 mutations associated with diffuse parenchymal lung diseases in children, Hum. Mol. Genet. 21 (4) (2012) 765–775.
[16] M. Griese, et al., Surfactant lipidomics in healthy children and childhood interstitial lung disease, PLoS One 10 (2) (2015) e0117985.
[17] N. Akil, A.J. Fischer, Surfactant deficiency syndrome in an infant with a C-terminal frame shift in ABCA3: a case report, Pediatr. Pulmonol. 53 (5) (2018) E12–E14.
[18] S. Kinting, et al., Potentiation of ABCA3 lipid transport function by ivacaftor and genistein, J. Cell. Mol. Med. 23 (8) (2019) 5225–5234.
[19] S. Kinting, et al., Functional rescue of misfolding ABCA3 mutations by small molecular correctors, Hum. Mol. Genet. 27 (6) (2018) 943–953.
[20] S. Hoppner, et al., Quantification of volume and lipid filling of intracellular vesicles carrying the ABCA3 transporter, Biochim Biophys Acta Mol Cell Res 1864 (12) (2017) 2330–2335.
[21] C.R. Gault, L.M. Obeid, Y.A. Hannun, An overview of sphingolipid metabolism: from synthesis to breakdown, Adv. Exp. Med. Biol. 688 (2010) 1–23.
[22] C.Y. Jao, et al., Metabolic labeling and direct imaging of choline phospholipids in vivo, Proc. Natl. Acad. Sci. U. S. A. 106 (36) (2009) 15332–15337.
[23] R. Aharoni, et al., Assessing remyelination - metabolic labeling of myelin in an animal model of multiple sclerosis, J. Neuroimmunol. 301 (2016) 7–11.
[24] A.A. Torrano, et al., A fast analysis method to quantify nanoparticle uptake on a single cell level, Nanomedicine (Lond) 8 (11) (2013) 1815–1828.
[25] A. Rodriguez-Gonzalez, et al., Inhibition of choline kinase as a specific cytotoxic strategy in oncogene-transformed cells, Oncogene 22 (55) (2003) 8803–8812.
[26] L.C. Dohmen, et al., Functional validation of ABCA3 as a miltefosine transporter in human macrophages: IMPACT ON INTRACELLULAR SURVIVAL OF LEISHMANIA (VIANNIA) PANAMENSIS, J. Biol. Chem. 291 (18) (2016) 9638–9647.
[27] S. Shulenin, et al., ABCA3 gene mutations in newborns with fatal surfactant deficiency, N. Engl. J. Med. 350 (13) (2004) 1296–1303.
[28] G. Chevalier, A.J. Collet, In vivo incorporation of choline- 3 H, leucine- 3 H and galactose- 3 H in alveolar type II pneumocytes in relation to surfactant synthesis. A quantitative radoautographic study in mouse by electron microscopy, Anat. Rec. 174 (3) (1972) 289–310.
[29] K. Osanai, et al., Pulmonary surfactant transport in alveolar type II cells, Respirology (11) (2006) S70–S73 Suppl.
[30] A. Suwabe, R.J. Mason, D.R. Voelker, Temporal segregation of surfactant secretion and lamellar body biogenesis in primary cultures of rat alveolar type II cells, Am. J. Respir. Cell Mol. Biol. 5 (1) (1991) 80–86.
[31] P.A. Stevens, J.R. Wright, J.A. Clements, Surfactant secretion and clearance in the newborn, J Appl Physiol (1985) 67 (4) (1989) 1597–1605.
[32] Z. Luo, et al., High-resolution optical molecular imaging of changes in choline metabolism in oral neoplasia, Transl. Oncol. 6 (1) (2013) 33–41.
[33] A.M. Di Guilmi, et al., Specific and spatial labeling of choline-containing teichoic acids in Streptococcus pneumoniae by click chemistry, Chem Commun (Camb) 53 (76) (2017) 10572–10575.
[34] J.M. Paper, T. Mukherjee, K. Schrick, Bioorthogonal click chemistry for fluorescence imaging of choline phospholipids in plants, Plant Methods 14 (2018) 31.
[35] N.M. Al-Saffar, et al., Noninvasive magnetic resonance spectroscopic pharmacodynamic markers of the choline kinase inhibitor MN58b in human carcinoma models, Cancer Res. 66 (1) (2006) 427–434.
[36] E.P. Kennedy, S.B. Weiss, The function of cytidine coenzymes in the biosynthesis of phospholipides, J. Biol. Chem. 222 (1) (1956) 193–214.
[37] F. Gibellini, T.K. Smith, The Kennedy pathway–De novo synthesis of phosphatidylethanolamine and phosphatidylcholine, IUBMB Life 62 (6) (2010) 414–428.
[38] J.G. Kay, et al., Phosphatidylserine dynamics in cellular membranes, Mol. Biol. Cell 23 (11) (2012) 2198–2212.
[39] R.J. Swain, et al., Assessment of cell line models of primary human cells by Raman spectral phenotyping, Biophys. J. 98 (8) (2010) 1703–1711.
[40] P. Mao, et al., Human alveolar epithelial type II cells in primary culture, Physiol Rep 3 (2) (2015).
[41] D. Steinbach, et al., ABCA3 as a possible cause of drug resistance in childhood acute myeloid leukemia, Clin. Cancer Res. 12 (14) (2006) 4357–4363 Pt 1.
[42] T. Aung, et al., Exosomal evasion of humoral immunotherapy in aggressive B-cell lymphoma modulated by ATP-binding cassette transporter A3, Proc. Natl. Acad. Sci. U. S. A. 108 (37) (2011) 15336–15341.
[43] S. Rahgozar, et al., mRNA expression profile of multidrug-resistant genes in acute lymphoblastic leukemia of children, a prognostic value for ABCA3 and ABCA2, Cancer Biol Ther 15 (1) (2014) 35–41.